

A New Quantitative Imaging Biomarker for Identifying Critical Coronary Artery Stenosis with Myocardial BOLD MRI

S. A. Tsaftaris^{1,2}, X. Zhou², D. Li^{2,3}, and R. Dharmakumar²

¹Electrical Engineering and Computer Science, Northwestern University, Evanston, IL, United States, ²Radiology, Northwestern University, Chicago, IL, United States, ³Biomedical Engineering, Northwestern University, Evanston, IL, United States

Introduction: Blood-oxygen-level dependent (BOLD) MRI may be used for detecting myocardial oxygenation changes secondary to coronary artery stenosis (CAS) (1-3). Under pharmacological stress, areas of the myocardium supplied by a stenotic coronary artery appear hypointense relative to healthy regions in BOLD images. Manual windowing is often required to visualize these changes and segmentation of the myocardium according to the American Heart Association's (AHA) recommendation is used to confirm and characterize the BOLD effect. However, the identification of critical (clinically significant) CAS on the basis of BOLD MRI has mostly been met with limited sensitivity. The purpose of this work is to present a fundamentally new direction for visualizing and quantifying regional myocardial BOLD signal changes. The proposed approach, tested on a canine model, identifies the affected territory of the myocardium based on a statistical framework, correlates strongly with reference flow measurements, and most importantly, leads to a significant increase in sensitivity to microvascular flow changes compared to previous approaches.

Methods: Imaging Studies: Short-axis 2D cine SSFP-based myocardial BOLD images were acquired in 7 dogs during rest (baseline) and under adenosine stress with and without left-circumflex (LCX) CAS (controlled with a surgically implanted hydraulic occluder) using a Siemens 1.5T scanner. Scan parameters were: resolution=1.2x1.2x6mm³; flip-angle=90°; and TR/TE=6.2/3.1ms. Fluorescent microspheres were infused to measure myocardial perfusion at different physiologic states. Following imaging studies, dogs were euthanized and the myocardial tissue was processed (in a segmental fashion) to ascertain perfusion. Segmental perfusion values were summed to obtain total flow (μ_F) for each slice (4). **Image Processing:** To have the largest myocardial surface for analysis, end-systolic (ES) images were identified in each study using an automated method (5) and their endo- and epicardial borders were traced. In the following, BA refers to baseline ES images, and STR refers to stress ES images (with or without CAS). Myocardial pixel intensities were collected from BA and the mean (μ) and variance (σ) of a location-scaled Student's t-distribution were found using maximum likelihood estimation. Based on the threshold $T = \mu - \sigma$, the largest contiguous hypointense region was identified (pixel intensity < T) and C_M the number of pixels in the region divided by the total number of pixels in the entire myocardium was computed for both BA and STR images. $Q_M(\text{STR}, \text{BA}) = C_M(\text{STR})/C_M(\text{BA})$, that is C_M ratios between BA and STR images, were also calculated. For comparison, the myocardial images were segmented according to the recommendation of AHA. The segments from the LCX territory were identified in rest and stress images and their intensities were averaged and normalized by the average intensity of the myocardium and denoted as $AHA_M(\text{STR})$ and $AHA_M(\text{BA})$, respectively, which were later used to compute $I_M(\text{STR}, \text{BA}) = AHA_M(\text{STR}) / AHA_M(\text{BA})$. Q_M and I_M were regressed with the ratio of microsphere flow $\rho = \mu_F(\text{STR}) / \mu_F(\text{BA})$. Given that a perfusion ratio between stress and rest of 2:1 (or below) leads to critical perfusion anomaly (6), corresponding thresholds for Q_M and I_M were identified, and the sensitivity of each metric (Q_M and I_M) for detecting critical CAS was assessed.

Results: A representative set of rest and adenosine stress (with and without LCX stenosis) ES images with hypointense regions automatically detected and color-coded are shown in Fig. 1. Scatter plots of Q_M and I_M against ρ and the corresponding regression lines are shown in Fig. 2. Q_M showed a stronger correlation than I_M with ρ . In particular, I_M showed a linear relation with ρ ($R^2 = 0.5$), while Q_M showed a stronger exponential ($R^2 = 0.8$) than linear ($R^2 = 0.7$) relation with ρ . True perfusion measurements revealed that the infliction of various LCX stenoses in the dogs led to 8 critical ($\rho \leq 2$, Actual Positives) and 9 non-critical ($\rho > 2$, Actual Negatives) perfusion changes. For $\rho \leq 2$, detection rules for Q_M and I_M were identified as: $Q_M \geq 2.1$ and $I_M \leq 0.94$ (see Fig. 2 legend for details). On the basis of these thresholds, the Q_M -based approach yielded 1 False Positive and 1 False Negative, while the I_M -based evaluation resulted in 2 False Positives and 4 False Negatives. Overall, the sensitivity of Q_M vs. I_M was 87% vs. 50%, respectively, and the specificity of Q_M vs. I_M was 89% vs 77%, respectively. The considerable sensitivity difference between the Q_M and I_M metrics is also attested by their rate of change relative to ρ at the respective detection thresholds; specifically, 1.1 (exponential fit) and 0.65 (linear fit) for Q_M vs. 0.03 for I_M .

Discussion & Conclusions: This study proposed, tested, and validated a statistical approach for identifying myocardial territories affected by CAS in adenosine stress images based on thresholds derived from rest images in canines. The percentage of hypointense pixels in the myocardium (C_M) was hypothesized to increase with the severity of CAS in relation to rest conditions. Results showed that the area-based metric, Q_M , introduced here as the ratio of C_M among stress and rest ES images, correlates strongly with microsphere flow measurements. More importantly, the proposed method provides an order of magnitude greater sensitivity for detecting microvascular flow changes (rate of change 1.1 for Q_M) compared to mean intensity metrics relying on segmental analysis (rate of change 0.03 for I_M , which is in agreement with other studies (2-3)). While the method can provide substantially greater detection sensitivity and specificity compared to previous approaches, additional improvements in sensitivity and specificity may require further improvements in imaging strategies. Nevertheless, the proposed method has the potential to not only rapidly determine the presence of oxygenation anomalies in the myocardium due to coronary artery disease, but also deliver an unbiased and quantitative imaging biomarker that can enable the assessment of the critical states of CAS on the basis of BOLD MRI. The method remains to be evaluated in humans.

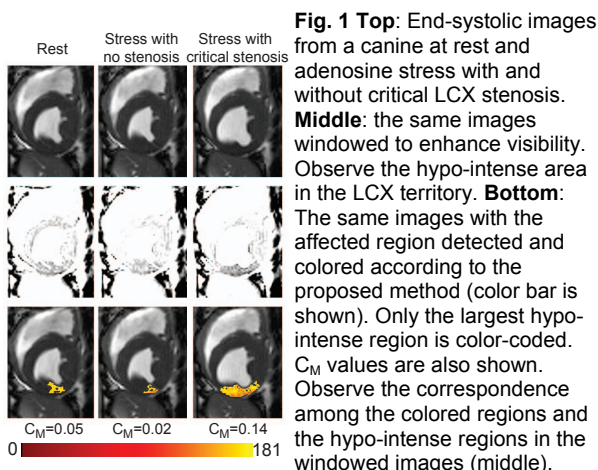


Fig. 1 Top: End-systolic images from a canine at rest and adenosine stress with and without critical LCX stenosis. **Middle:** the same images windowed to enhance visibility. Observe the hypo-intense area in the LCX territory. **Bottom:** The same images with the affected region detected and colored according to the proposed method (color bar is shown). Only the largest hypo-intense region is color-coded. C_M values are also shown. Observe the correspondence among the colored regions and the hypo-intense regions in the windowed images (middle).

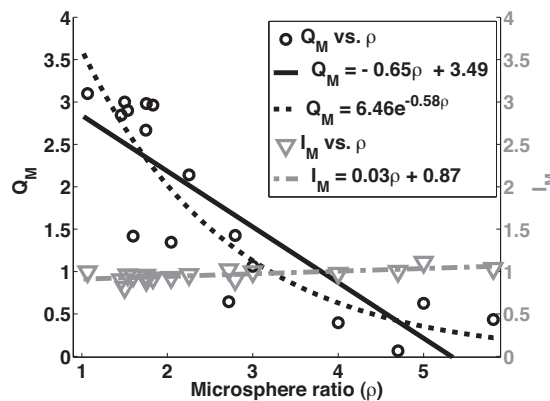


Fig. 2 Scatter plots of Q_M and I_M vs. microsphere ratio measurements (ρ) as described in text are shown. Linear ($R^2=0.7$) and exponential ($R^2=0.8$) fits of Q_M and linear fit ($R^2=0.5$) of I_M vs. ρ are also shown. Note that the rate of change of Q_M relative to ρ is more than an order of magnitude greater than that of I_M . From the fits, for $\rho=2$ (critical stenosis), the values of Q_M (exponential fit) and I_M are 2.1 and 0.94, respectively. These values were used as thresholds for the sensitivity and specificity analysis.

References: (1) Friedrich et al., *Circ* 108:2219-2223(2003); (2) Shea et al., *Radiology* 236(2):503-509(2005); (3) Dharmakumar et al., *Inv. Rad.* 42(3):18 0-188(2007); (4) Wilke et al., *Magn. Res. Q.*, 10(4):249-286(1994); (5) Tsaftaris et al., *ISMRM 2009 #3748*; (6) Klocke et al., *Circ* 104:2412-2416 (2001).